"Outer-Sphere to Inner-Sphere" Redox Cycling for Ultrasensitive Immunosensors

ARTICLE *in* ANALYTICAL CHEMISTRY · DECEMBER 2011

Impact Factor: 5.64 · DOI: 10.1021/ac202638y · Source: PubMed

3 AUTHORS, INCLUDING:

Muhammad Rajibul Haque Akanda
Jagannath University - Bangladesh
8 PUBLICATIONS **136** CITATIONS
SEE PROFILE

Haesik Yang
Pusan National University
114 PUBLICATIONS **2,445** CITATIONS
SEE PROFILE

analytical chemistry

Article

pubs.acs.org/ac

"Outer-Sphere to Inner-Sphere" Redox Cycling for Ultrasensitive Immunosensors

Md. Rajibul Akanda, Yu-Lim Choe, and Haesik Yang*

Department of Chemistry and Chemistry Institute for Functional Materials, Pusan National University, Busan 609-735, Korea

Supporting Information

ABSTRACT: This paper reports chemical−chemical (CC) and electrochemical−chemical−chemical (ECC) redox cycling, for use in ultrasensitive biosensor applications. A triple chemical amplification approach using an enzymatic reaction, CC redox cycling, and ECC redox cycling is applied toward electrochemical immunosensors of cardiac troponin I. An enzymatic reaction, in which alkaline phosphatase converts 4-aminophenyl phosphate to 4-aminophenol (AP), triggers CC redox cycling in the presence of an oxidant and a reductant, and electrochemical signals are measured with ECC redox cycling after an incubation period of time in an air-saturated solution. To obtain high, selective, and reproducible redox cycling without using redox enzymes, two redox reactions [the reaction between AP and the oxidant and the reaction between the oxidized form of AP (4-quinone imine, QI) and the reductant] should be fast, but an unwanted reaction between the oxidant and reductant should be very slow. Because species that undergo outer-sphere reactions (OSR-philic species) react slowly with species that undergo inner-sphere reactions (ISR-philic species), highly OSR-philic $Ru(NH_3)_6^{3+}$ and highly ISR-philic tris(2-carboxyethyl)phosphine (TCEP) are chosen as the oxidant and reductant, respectively. The OSR- and ISR-philic QI/AP couple allows fast redox reactions with both the OSR-philic $Ru(NH_3)_6^{3+}$ and the ISR-philic TCEP. Highly OSR-philic indium−tin oxide (ITO) electrodes minimize unwanted electrochemical reactions with highly ISR-philic species. Although the formal potential of the $Ru(NH_3)_6^{3+}/Ru(NH_3)_6^{2+}$ couple is lower than that of the QI/AP couple, the endergonic reaction between $Ru(NH_3)_6^{3+}$ and AP is driven by the highly exergonic reaction between TCEP and QI (via a coupled reaction mechanism). Overall, the "outer-sphere to inner-sphere" redox cycling in the order of highly OSR-philic ITO, highly OSR-philic $Ru(NH_3)_6^{3+}/Ru(NH_3)_6^{2+}$ couple, OSR- and ISR-philic QI/AP couple, and highly ISR-philic TCEP allows high, selective, and reproducible signal amplification. The electrochemical data obtained by chronocoulometry permit a lower detection limits than those obtained by cyclic voltammetry. The detection limit of an immunosensor for troponin I in serum, calculated from the anodic charges in chronocoulometry, is ca. 10 fg/mL.

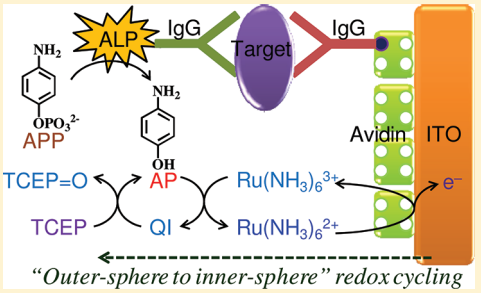

Signal amplification, which is essential for sensitive and fast detection, can be achieved by generating many targets or signaling species from one target species (chemical amplification) or by enhancing the sensitivity of a transducer (physical amplification).[1−11] Generally, chemical amplification is preferred in highly sensitive detection because it raises the signal level without significantly changing the background level, that is, it yields a high signal-to-background ratio.[1,2,9−11] For more sensitive detection, it is crucial to attain high, selective, and reproducible chemical amplification.

High chemical amplification can be obtained using a catalytic reaction (single amplification)[2,6,8] or a catalytic reaction plus a redox-cycling reaction (double amplification)[1,3,4,12−18] in a biosensor using catalytic labels, such as enzymes[19,20] or nanocatalysts[12] (Figure 1). A catalytic reaction includes an enzymatic reaction[19,20] (reaction 1-a of Figure 1) and a nanocatalytic reaction[12] (reaction 1-b of Figure 1), and a redox-cycling reaction includes electrochemical−electrochemical (EE) redox cycling[3,4,21,22] (reaction 2-a of Figure 1) and electrochemical−chemical (EC) redox cycling[13−18,23,24] (reaction 2-b of Figure 1). In EE redox cycling, a signaling species is redox-cycled by two electrodes, whereas in EC redox cycling, it is cycled by an electrode and a reducing (or oxidizing) agent. Another possible redox-cycling approach is chemical−chemical (CC) redox cycling (reaction 2-c of Figure 1),[1,25] which is used for the trace analysis of redox metal ions and is called the kinetic−catalytic method.[26−28] In many cases, EC and CC redox cycling requires redox enzymes that allow selective and fast redox reactions.[1,13−16,25] Especially in biosensors, there is no report of achieving CC redox cycling without using redox enzymes.

Most chemical amplification occurs in conjunction with unwanted reactions that decrease the signal level or increase the background level. Therefore, it is important to obtain selective chemical amplification that facilitates minimal unwanted reactions. Enzymatic reactions readily allow selective and high chemical amplification under mild conditions.[2,8] However, EC and CC redox cycling (obtained without using redox enzymes), which must generally be performed under less mild conditions,

Received: October 6, 2011
Accepted: December 13, 2011
Published: December 30, 2011

   dx.doi.org/10.1021/ac202638y | *Anal. Chem.* 2012, 84, 1049−1055

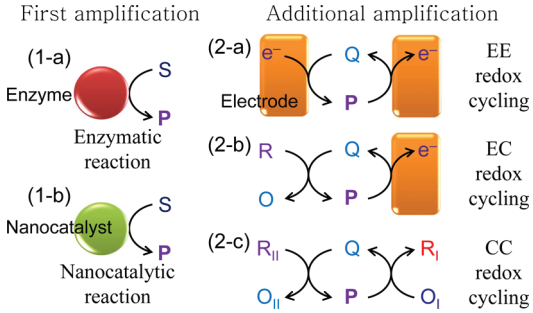

Figure 1. Schematic representation of signal-amplification methods in electrochemical biosensors: (1) catalytic reactions and (2) redox-cycling reactions. Catalytic reactions include (1-a) an enzymatic reaction and (1-b) a nanocatalytic reaction. Redox-cycling reactions include (2-a) EE redox cycling, (2-b) EC redox cycling, and (2-c) CC redox cycling. S, enzyme substrate; P, enzyme product; Q, oxidized form of P; O_I, oxidant; R_I, reduced form of O_I; R, R_{II}, reductant; O, O_{II}, oxidized form of R, R_{II}.

could be accompanied by various unwanted reactions, for example, the reaction between R_{II} and O_I in reaction 2-c of Figure 1. As many unwanted reactions are thermodynamically favorable; they must be kinetically minimized. Accordingly, the chemical species involved in redox cycling should be properly chosen in view of kinetic considerations.[26]

The kinetics of redox reactions depend on the redox species involved and the type of electron transfer.[29−34] Taube articulated that the electron transfer between inorganic coordination complexes follows two pathways including outer-sphere and inner-sphere electron transfer.[33,34] Kochi and co-workers proposed that the electron transfer between an organic electron donor and an acceptor can also be classified into outer-sphere and inner-sphere electron transfer, depending on the degree of electronic coupling (orbital overlap), and that outer-sphere electron transfer occurs with no or very little electronic coupling between the donor and acceptor.[30−32] The concept of outer-sphere and inner-sphere electron transfer can be extended to electrode reactions.[35] In the area of dye-sensitized solar cells, the term "outer-sphere redox couple" and "inner-sphere redox couple" have been commonly employed to describe the type of electron transfer for ferrocenium/ferrocene couple and I_3^-/I^- couple, respectively.[36,37] From such views, redox species can be classified into species that undergo inner-sphere reactions (ISR-philic species) and species that undergo outer-sphere reactions (OSR-philic species). Many redox species are both ISR-philic and OSR-philic, and they can undergo inner-sphere and outer-sphere reactions. However, highly OSR-philic redox species are mainly reduced/oxidized by outer-sphere reactions, whereas highly ISR-philic redox species are mainly reduced/oxidized by inner-sphere reactions. In reaction 2-c of Figure 1, if one of R_{II} and O_I is highly OSR-philic and the other is highly ISR-philic, and if P and Q are both OSR-philic and ISR-philic, CC redox cycling may well occur in conjunction with a very slow unwanted reaction between R_{II} and O_I.

The reproducibility of chemical amplification depends strongly on the reaction temperature and the stability of the species involved in a catalytic reaction and redox cycling. Accordingly, it is essential to maintain a constant temperature during the chemical amplification step. Moreover, to achieve a reproducible sensor response, the temperature of biospecific binding events (for example, antigen−antibody binding) must be properly adjusted.[18] The stability of most redox species in aqueous solutions is influenced by their reactions with O_2 because the reactions are thermodynamically highly favorable. Therefore, redox species that react kinetically slowly with O_2 are preferred for achieving reproducible chemical amplification.

The authors reported previously that double chemical amplification using an enzymatic reaction and an EC redox cycling allowed the ultrasensitive detection of proteins.[17,18] In this study, the authors report the first introduction of CC and electrochemical−chemical−chemical (ECC) redox cycling that is obtained without using redox enzymes. Optimum conditions for the CC and ECC redox cycling were investigated and applied toward the detection of mouse IgG and troponin I.

EXPERIMENTAL SECTION

All the experimental information is available in the Supporting Information.

RESULTS AND DISCUSSION

Evaluation of a CC and ECC Redox-Cycling System. In this study, CC and ECC redox-cycling reactions (reactions i and ii of Figure 2a) were combined with an enzymatic reaction (reaction 1-a of Figure 1). For this purpose, alkaline

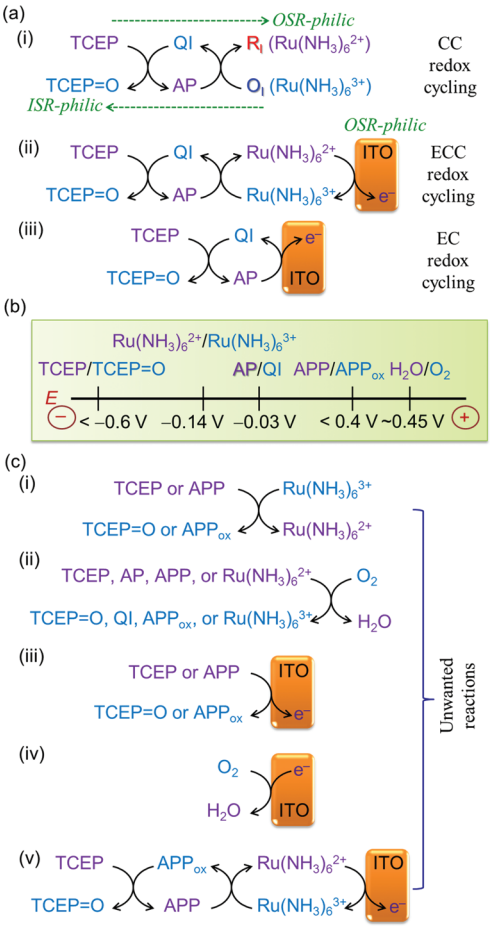

Figure 2. (a) Possible redox-cycling reactions: (i) CC redox cycling, (ii) ECC redox cycling, (iii) and EC redox cycling. (b) Relative positions of estimated formal potentials (vs Ag/AgCl) of the redox couples that may be involved in redox-cycling reactions and unwanted reactions. The relative positions are explained in the Supporting Information. (c) Possible unwanted reactions.

dx.doi.org/10.1021/ac202638y | Anal. Chem. 2012, 84, 1049−1055

phosphatase (ALP) was chosen as an enzyme for the enzymatic reaction, as ALP shows high activity and long-term stability.[38] Next, the authors needed to select a proper CC redox-cycling system that consists of an ALP product (P), a reductant (R_{II}), and an oxidant (O_I) (reaction 2-c of Figure 1). In our previous study, tris(2-carboxyethyl)phosphine (TCEP) was used for EC redox cycling, because it allowed fast EC redox cycling, it was slowly electrooxidized at indium−tin oxide (ITO) electrodes, and it was resistant to oxidation by O_2.[18,39] For the same reasons, TCEP was selected as a reductant (R_{II}) for the CC and ECC redox cycling. Of several ALP products, 4-aminophenol (AP) was chosen as an ALP product because AP redox cycling by TCEP allows higher electrochemical currents.[18] To search for an oxidant for the CC and ECC redox cycling, the following requisites were considered: (i) from a thermodynamic perspective, the formal potential of an oxidant (O_I) should be much higher than that of the reductant (TCEP); (ii) from a kinetic perspective, the oxidant (O_I) should be highly OSR-philic.

Figure 2b shows the relative positions of the formal potentials of the redox couples that may be involved in the CC and ECC redox cycling and the unwanted reactions. O_2 reduction is included in Figure 2b, as its formal potential is sufficiently high to oxidize most reduced species thermodynamically. The formal potentials increase in the sequence of TCEP═O (oxidized form of TCEP)/TCEP, QI (4-quinone imine)/AP, APP_{ox} (oxidized form of 4-aminophenyl phosphate (APP))/APP, and O_2/H_2O (see the Supporting Information). For selective CC and ECC redox cycling, O_I should react with AP but not with APP. The formal potential of O_I/R_I (reduced form of O_I) should be higher than that of TCEP═O/TCEP (Figure 2b).

The oxidation of TCEP to TCEP═O requires double-bond formation (with oxygen atom of water)[39] that cannot be achieved by an outer-sphere reaction mechanism. Moreover, the rate of reduction of an oxidized species by TCEP depends strongly on the type of the oxidized species. Both results indicate that TCEP is highly ISR-philic. Highly ISR-philic redox species are mainly reduced/oxidized by inner-sphere reactions, whereas highly OSR-philic redox species are mainly reduced/oxidized by outer-sphere reactions. In general, the reaction between a highly ISR-philic species and a highly OSR-philic species is very slow. In this regard, highly OSR-philic O_I was required to achieve a slow reaction with highly ISR-philic TCEP. Common outer-sphere redox species that allow high electron-transfer rates, ($Ru(NH_3)_6^{3+}$, $Fe(CN)_6^{3-}$, and ferrocenium ion),[40,41] can be used as highly OSR-philic O_I. However, $Fe(CN)_6^{3-}$ and ferrocenium ion were not appropriate, because $Fe(CN)_6^{3-}$ reacted rapidly with TCEP and ferrocenium ion is unstable in aqueous solutions, especially those containing chloride ion.[42] Because $Ru(NH_3)_6^{3+}$ reacted very slowly with TCEP and $Ru(NH_3)_6^{3+}$ does not react with ALP,[43] a CC and ECC redox-cycling system using $Ru(NH_3)_6^{3+}$ as the O_I (reactions i and ii of Figure 2a) was considered.

The ECC redox cycling of reaction ii of Figure 2a includes the CC redox cycling of reaction i of Figure 2a. Therefore, the occurrence of the CC redox cycling can be investigated by checking the ECC redox cycling. To compare the relative positions of the formal potentials of QI/AP and $Ru(NH_3)_6^{3+}$/$Ru(NH_3)_6^{2+}$, cyclic voltammograms of AP and $Ru(NH_3)_6^{2+}$ were obtained at a glassy carbon electrode (Figure S1 in the Supporting Information). Judging from the anodic and cathodic peak potentials, the formal potential of $Ru(NH_3)_6^{3+}$/$Ru(NH_3)_6^{2+}$ was approximately 110 mV lower than that of QI/AP. In this situation, only a small portion of AP could be oxidized by $Ru(NH_3)_6^{3+}$, and efficient redox cycling may not be obtainable. To check for this adverse possibility, a cyclic voltammogram obtained in a solution containing $Ru(NH_3)_6^{2+}$ and AP (curve iii of Figure 3a) at a bare ITO electrode was compared with that in a solution containing $Ru(NH_3)_6^{2+}$ only

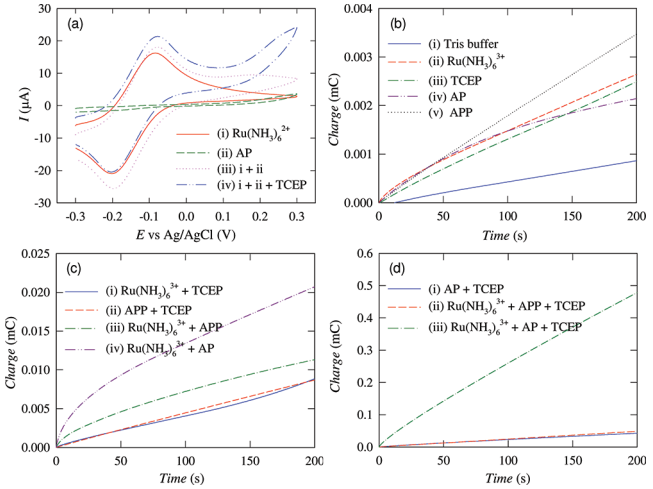

Figure 3. (a) Cyclic voltammogram obtained in Tris-buffer solutions (pH 8.9) containing 1.0 mM $Ru(NH_3)_6^{2+}$, 0.10 mM AP, and/or 2.0 mM TCEP at bare ITO electrodes after argon purging for 10 min. (b−d) Chronocoulograms obtained in various air-saturated Tris-buffer solutions (pH 8.9) containing 1.0 mM $Ru(NH_3)_6^{3+}$, 0.10 mM AP, and/or 2.0 mM TCEP at 0.05 V at ITO electrodes just after mixing. An AP concentration of 0.10 mM instead of higher concentrations was used to show that the signal-to-background ratios are high in the presence of AP, even under the condition that $Ru(NH_3)_6^{3+}$, TCEP, and APP increase background levels.

(curve i of Figure 3a). The oxidation currents of $Ru(NH_3)_6^{2+}$ in the presence of AP during the anodic scan, especially above 0.0 V (curve iii of Figure 3a), were slightly higher than those in the absence (curve i of Figure 3a). Considering that the oxidation currents of AP were not considerable over this range of potentials (curve ii of Figure 3a), the higher currents indicated that $Ru(NH_3)_6^{2+}$ was regenerated by the reduction of $Ru(NH_3)_6^{3+}$ by AP. In a solution containing $Ru(NH_3)_6^{2+}$, AP, and TCEP, the oxidation currents of $Ru(NH_3)_6^{2+}$ were much higher (curve iv of Figure 3a), indicating that $Ru(NH_3)_6^{2+}$ was rapidly regenerated by the redox cycling of reaction ii of Figure 2a. Cyclic voltammograms were also obtained in a solution containing $Ru(NH_3)_6^{3+}$ (instead of $Ru(NH_3)_6^{2+}$), AP, and TCEP (Figure S2 in the Supporting Information). To avoid the electrochemical generation of $Ru(NH_3)_6^{2+}$, an initial potential of 0.0 V was chosen in cyclic voltammetry. The initial anodic current (31 μA) in the voltammogram obtained 10 min after mixing the three solutions of $Ru(NH_3)_6^{3+}$, AP, and TCEP was much higher than that (10 μA) measured just after mixing. This result suggested that many $Ru(NH_3)_6^{2+}$ complexes were generated during the 10 min incubation period of time via the CC redox cycling of reaction i of Figure 2a. This result clearly showed that the CC redox cycling occurred, although the formal potential of the $Ru(NH_3)_6^{3+}$/$Ru(NH_3)_6^{2+}$ couple was lower than that of QI/AP. This finding can be understood in terms of a "coupled reaction" mechanism.[46] Because the formal potential of TCEP═O/TCEP is much lower than the

dx.doi.org/10.1021/ac202638y | Anal. Chem. 2012, 84, 1049−1055

potentials of $Ru(NH_3)_6^{3+}/Ru(NH_3)_6^{2+}$ and QI/AP, the endergonic reaction between $Ru(NH_3)_6^{3+}$ and AP is driven by the highly exergonic reaction between TCEP and QI. As a result, the overall CC redox-cycling reaction becomes highly exergonic.

To investigate whether the CC and ECC redox cycling is sufficiently fast to allow a high signal-to-background ratio, chronocoulograms were obtained in various solutions containing $Ru(NH_3)_6^{3+}$, AP, and/or TCEP at ITO electrodes (Figure 3b–d). Chronocoulograms depend on the applied potential, which should be much higher than the formal potential of $Ru(NH_3)_6^{3+}/Ru(NH_3)_6^{2+}$ in order to prevent the electroreduction of $Ru(NH_3)_6^{3+}$. However, when the applied potential is too high, the extent of electrooxidation of $Ru(NH_3)_6^{3+}$ to Ru^{IV} complex is considerable.[44,45] To obtain high anodic charges in the presence of AP along with low charges in the absence of AP, an applied potential of 0.05 V was found to be optimal (Figure S3 in the Supporting Information).

The anodic charges in a solution containing $Ru(NH_3)_6^{3+}$ and AP (curve iv of Figure 3c) were much higher than those in a solution containing $Ru(NH_3)_6^{3+}$ only (curve ii of Figure 3b). The difference between the two anodic charges is largely due to the electrooxidation of the $Ru(NH_3)_6^{2+}$ generated by AP, not the electrooxidation of AP, because the anodic charges of AP were not considerable at this potential (curve iv of Figure 3b). The anodic charges in a solution containing $Ru(NH_3)_6^{3+}$, AP, and TCEP (curve iii of Figure 3d) were significantly higher than those in a solution containing $Ru(NH_3)_6^{3+}$ and AP (curve iv of Figure 3c) and those in a solution containing AP and TCEP (curve i of Figure 3d). These results clearly showed that the ECC redox cycling (reaction ii of Figure 2a) readily occurred and that the ECC redox cycling allowed higher electrochemical signals than the EC redox cycling (reaction iii of Figure 2a).

The reaction between $Ru(NH_3)_6^{3+}$ (oxidant) and TCEP (reductant) (reaction i of Figure 2c) could significantly increase background levels. The anodic charges in a solution containing $Ru(NH_3)_6^{3+}$ and TCEP (curve i of Figure 3c) were higher than the total values of the charges in a solution containing $Ru(NH_3)_6^{3+}$ only (curve ii of Figure 3b) and the charges in a solution containing TCEP only (curve iii of Figure 3b). The higher charges were due to the electrooxidation of $Ru(NH_3)_6^{2+}$ generated by the reaction between $Ru(NH_3)_6^{3+}$ and TCEP. Nevertheless, the charges in a solution containing $Ru(NH_3)_6^{3+}$ and TCEP (curve i of Figure 3c) were much lower than those in a solution containing $Ru(NH_3)_6^{3+}$, AP, and TCEP (curve iii of Figure 3d). This result clearly showed that the redox reaction between highly OSR-philic $Ru(NH_3)_6^{2+}$ and highly ISR-philic TCEP was negligibly slow compared to the ECC redox cycling.

O_2 can react with TCEP, AP, APP, and $Ru(NH_3)_6^{2+}$ (reaction ii of Figure 2c).[39,47,48] These reactions can significantly reduce the efficiency of redox cycling. In a chronoamperogram obtained in a solution containing $Ru(NH_3)_6^{3+}$, AP, and TCEP (Figure S4 in the Supporting Information), the currents approached a steady-state behavior after an initial current decrease, indicating that the redox cycling occurred stably. This result showed that all species involved in the redox cycling were quite stable during cycling.

Organic molecules containing planar (aromatic or olefinic) redox centers, such as AP and QI, can undergo both inner-sphere and outer-sphere reactions,[29,32] and they are ISR-philic and OSR-philic. Therefore, both a fast reaction between QI and ISR-philic TCEP and a fast reaction between AP and OSR-philic $Ru(NH_3)_6^{3+}$ were possible. Moreover, the high stability of AP and QI contributed to the stable redox cycling. If QI was unstable, the ECC redox cycling would rapidly decrease with time and stop in a certain period of time.

Many unwanted reactions could potentially occur at ITO electrodes. TCEP oxidation (reaction iii of Figure 2c) and O_2 reduction (reaction iv of Figure 2c) could vary the background levels. Because ITO electrodes have low electrocatalytic activities, inner-sphere reactions do not occur extensively at ITO electrodes, although outer-sphere reactions do.[17,18,49,50] This result suggests that ITO electrodes are highly OSR-philic. Accordingly, the electrochemical reactions of highly ISR-philic TCEP and O_2 were negligible at highly OSR-philic ITO electrodes, provided the applied potentials were not extreme.

The reaction between $Ru(NH_3)_6^{3+}$ and APP in the presence of TCEP could also occur by a "coupled reaction" mechanism (reaction v of Figure 2c), although the formal potential of $Ru(NH_3)_6^{3+}/Ru(NH_3)_6^{2+}$ was much lower than that of APP_{ox}/APP. Thus, the anodic charges in a solution containing $Ru(NH_3)_6^{3+}$, APP, and TCEP (curve ii of Figure 3d) were much higher than the total values of the anodic charges in a solution containing $Ru(NH_3)_6^{3+}$ and APP (curve iii of Figure 3c) and the anodic charges in a solution containing TCEP only (curve iii of Figure 3b). Nevertheless, the charges in a solution containing $Ru(NH_3)_6^{3+}$, APP, and TCEP (curve ii of Figure 3d) were much lower than those in a solution containing $Ru(NH_3)_6^{3+}$, AP, and TCEP (curve iii of Figure 3d).

The charges measured at 100 s in Figure 3b–d are shown in Table 1. The difference between the charge for AP and the charge for none corresponds to the charge due to AP electrooxidation in the absence of redox cycling. The difference between the charge for AP + TCEP and the charge for TCEP corresponds to the charge mainly due to the EC redox cycling (reaction iii of Figure 2a). It indicates that the AP signal in the presence of TCEP was increased by an amplification factor of ca. 21. The difference between the charge for $Ru(NH_3)_6^{3+}$ + AP + TCEP and the charge for $Ru(NH_3)_6^{3+}$ + TCEP corresponds to the charge mainly due to the ECC and EC redox cycling (reaction ii of Figure 2a). It indicates that the AP signal in the presence of TCEP and $Ru(NH_3)_6^{3+}$ was increased by an amplification factor of ca. 240.

Table 1. Charges Obtained at 100 s in Figure 3b–d

components	charge (mC)	difference (mC)	amplification factor
none (curve i of Figure 3b)	0.43	1.05	1
AP (curve iv of Figure 3b)	1.48		
TCEP (curve iii of Figure 3b)	1.31	21.8	21
AP + TCEP (curve i of Figure 3d)	23.1		
$Ru(NH_3)_6^{3+}$ + TCEP (curve ii of Figure 3c)	4.05	256	240
$Ru(NH_3)_6^{3+}$ + AP + TCEP (curve iii of Figure 3d)	260		

Overall, the CC and ECC redox cycling was sufficiently fast to obtain a high signal-to-background ratio, although many slow unwanted reactions took place simultaneously. Three redox-cycling reactions (CC, ECC, and EC redox cycling) took place, but ECC redox cycling largely contributed to electrochemical signals (chronocoulometric data) (see the Supporting Information and Figure S5). The "outer-sphere to inner-sphere" redox cycling occurred in the order of highly OSR-philic ITO, highly OSR-philic $Ru(NH_3)_6^{3+}/Ru(NH_3)_6^{2+}$ couple, OSR- and

dx.doi.org/10.1021/ac202638y | Anal. Chem. 2012, 84, 1049–1055

ISR-philic QI/AP couple, and highly ISR-philic TCEP (reaction ii of Figure 2c). Importantly, the CC and ECC redox cycling were obtained without using any redox enzymes that allow selective and fast redox reactions, and they were achieved in air-saturated solutions without removing oxygen.

Immunosensors Using CC and ECC Redox Cycling. The authors applied CC and ECC redox cycling to the detection of mouse IgG and troponin I, and determined detection limits of the immunosensors. To investigate the effects of CC and ECC redox cycling, the detection limit for mouse IgG in the presence of ECC redox cycling was compared with that in the presence of EC redox cycling. It is required to use an optimum set of $Ru(NH_3)_6^{3+}$, TCEP, and APP concentrations to obtain high signal amplification and to minimize unwanted reactions. However, we did not fully optimize the set of concentrations. It was considered that millimolar concentrations of ALP substrate and 2 mM TCEP are good for enzymatic reaction and redox cycling, respectively.[18]

Figure 4a shows a schematic diagram of an immunosensor (using enzymatic amplification and EC redox cycling) that does not employ CC and ECC redox cycling. Figure 5a shows cyclic

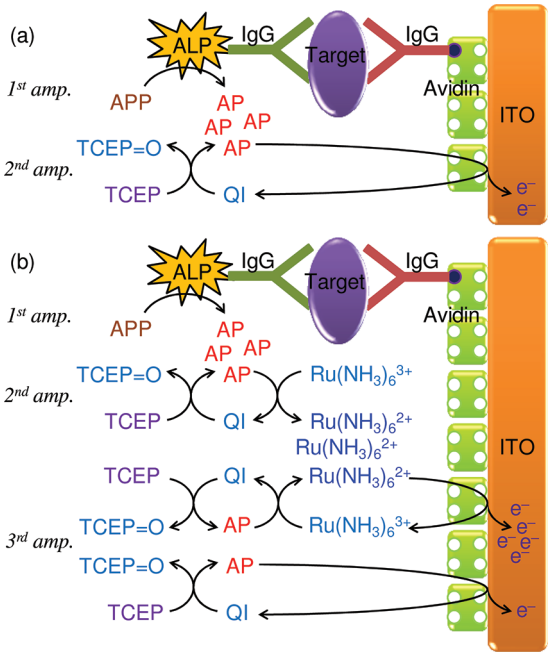

Figure 4. (a) Schematic representation of an electrochemical immunosensor using a double chemical amplification method: enzymatic reaction (first amplification) and EC redox cycling (second amplification). (b) Schematic representation of an electrochemical immunosensor using a triple chemical amplification method based on enzymatic reaction (first amplification), CC redox cycling (second amplification), and ECC and EC redox cycling (third amplification).

voltammograms obtained with an immunosensor of mouse IgG employing this scheme. No peak for AP electrooxidation was observed up to 0.4 V at the immunosensing electrodes, although an anodic peak was observed around 0.0 V at glassy carbon electrodes (Figure S1 in the Supporting Information). Moreover, background levels were considerable near and above 0.4 V because of APP electrooxidation.[51] When a calibration curve in Figure 5b was drawn using the current data recorded at 0.3 V during the anodic scan, all data were subtracted by the

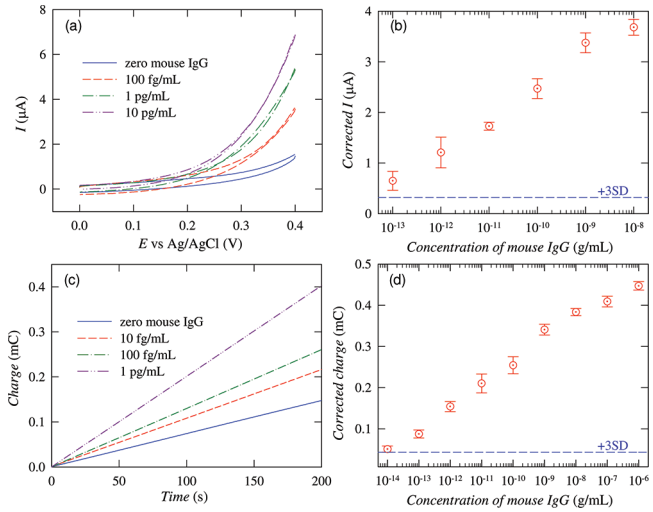

Figure 5. Results of the immunosensing experiments (using the scheme of Figure 4a) that were carried out with different concentrations of mouse IgG. (a) Cyclic voltammograms obtained (at a scan rate of 20 mV/s) in a Tris-buffer solution (pH 8.9) containing 1.0 mM APP and 2.0 mM TCEP after a 10 min incubation. (c) Chronocoulograms obtained at 0.3 V in a Tris-buffer solution (pH 8.9) containing 1.0 mM APP and 2.0 mM TCEP after a 10 min incubation. (b) Calibration plot: concentration dependence of the current at 0.3 V in panel a. (d) Calibration plot: concentration dependence of the charge at 100 s in panel c. All our immunosensing experiments were carried out with three different sensing electrodes for the same assay sample. All data were subtracted by the mean value at a concentration of zero determined by seven measurements. The dashed line corresponds to 3 times the standard deviation (SD) of the charge at a concentration of zero. The error bars represent the SD of three measurements.

mean current at a concentration of zero determined by seven measurements (0.63 μA). The standard deviation (SD) of the mean current was 0.11 μA, and the relative standard deviation (RSD) was 17%. The dashed line in Figure 5b corresponds to 3 times the SD, and the estimated detection limit was ca. 100 fg/mL.

In chronocoulometry,[52] the data integrated over a given period of time are used as sensor signals, whereas in cyclic voltammetry and chronoamperometry, the data measured at a given time are used. Accordingly, in many cases, the signals obtained by chronocoulometry are more reproducible than those obtained by cyclic voltammetry and chronoamperometry. Capacitive charging current in cyclic voltammetry is one of major sources of increased background levels in electrochemical sensors. In chronocoulometry, however, the influence of capacitive charging current can be significantly reduced if the measurement period is sufficiently long. Figure 5c shows chronocoulograms obtained at 0.3 V using the scheme shown in Figure 4a. The mean charge at 100 s at a concentration of zero was 50 μC, the SD was 14 μC, and the RSD was 28%. When a calibration curve was drawn using the charge data recorded at 100 s, the calculated detection limit was ca. 10 fg/mL (Figure 5d), which was 10-fold lower than that measured in cyclic voltammetry (Figure 5b).

Figure 4b shows a schematic diagram of an immunosensor that employs CC and ECC redox cycling. An enzymatic reaction generated many APs (first amplification), CC redox cycling generated many $Ru(NH_3)_6^{2+}$ complexes (second amplification), and ECC and EC redox cycling increased the

dx.doi.org/10.1021/ac202638y | Anal. Chem. 2012, 84, 1049–1055

electrochemical signals (third amplification). Although CC and EC redox cycling contributes to electrochemical signals, ECC redox cycling largely contributes when the charge is measured at 100 s. The mean charge at 100 s at a concentration of zero was 130 μC, the SD was 18 μC, and the RSD was 14% (Figure 6a). The estimated detection limit obtained using this scheme

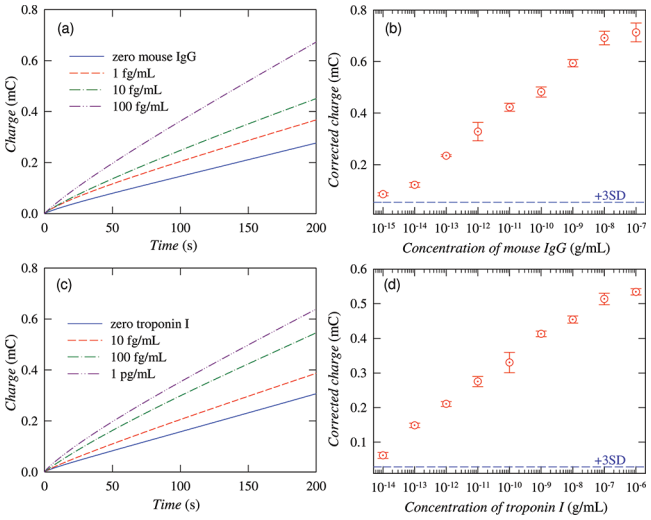

Figure 6. (a and b) Results of the immunosensing experiments (using the scheme of Figure 4b) that were carried out with different concentrations of mouse IgG; (c and d) results of the immunosensing experiments (using the scheme of Figure 4b) that were carried out with different concentrations of troponin I in human serum. (a and c) Chronocoulograms obtained at 0.05 V in a Tris-buffer solution (pH 8.9) containing 1.0 mM $Ru(NH_3)_6^{3+}$, 1.0 mM APP, and 2.0 mM TCEP after a 10 min incubation. (b) Calibration plot for the detection of mouse IgG: concentration dependence of the charge at 100 s in panel a. (d) Calibration plot for the detection of troponin I: concentration dependence of the charge at 100 s in panel c. All our immunosensing experiments were carried out with three different sensing electrodes for the same assay sample. All data were subtracted by the mean value at a concentration of zero determined by seven measurements. The dashed line corresponds to 3 times the standard deviation (SD) of the charge at a concentration of zero. The error bars represent the SD of three measurements.

was ca. 1 fg/mL (Figure 6b), which was 10-fold lower than that obtained in the presence of only EC redox cycling (Figure 5d). This result clearly showed that the ECC redox cycling facilitated obtaining high signal amplification, that is, a low detection limit.

When the CC and ECC redox cycling was applied to the detection of troponin I (molecular weight = 24 kDa),[53] the estimated detection limit was ca. 10 fg/mL (Figure 6, parts c and d), which corresponds to 400 aM. Importantly, troponin I could be detected over a wide range of concentrations, from 10 fg/mL to 10 ng/mL. Figure S6 in the Supporting Information shows seven chronocoulometric data sets obtained at a concentration of zero. The mean charge at 100 s was 150 μC, the SD was 10 μC, and the RSD was 7% (Figure 6c), indicating that the data were highly reproducible.

The detection limit for mouse IgG (1 fg/mL) is comparable to the lowest limits of recent ultrasensitive electrochemical sensors.[18,54] In the case of troponin I, the detection limit (10 fg/mL) is similar to that of our previous sensor[18] and much lower than those of other electrochemical sensors (2 and 4 pg/mL).[55,56]

CONCLUSIONS

An ultrasensitive immunosensing method employing CC and ECC redox cycling was developed without using redox enzymes. High chemical amplification was achieved using a triple amplification approach based on an enzymatic reaction, CC redox cycling, and ECC redox cycling. The "outer-sphere to inner-sphere" redox cycling enabled us to obtain high, selective, and reproducible signal amplification. Importantly, the sequential electron transfer in the redox cycling did not require modification of the low electrocatalytic ITO electrodes with electrocatalytic or electron-mediating materials. The immunosensing procedures developed here are the same as that used in conventional enzyme-based immunosensor procedures except for the simple addition of an oxidant $Ru(NH_3)_6^{3+}$ and a reductant TCEP. This similarity, along with the simple preparation and ultrasensitivity, renders this immunosensing method practical and appealing.

ASSOCIATED CONTENT

Supporting Information

More supporting data. This material is available free of charge via the Internet at http://pubs.acs.org.

AUTHOR INFORMATION

Corresponding Author

*E-mail: hyang@pusan.ac.kr.

ACKNOWLEDGMENTS

This research was supported by the Public Welfare & Safety Research Program (2010-0020772), the Basic Science Research Program (2009-0085182 and 2009-0072062), and the Nano/Bio Science & Technology Program (2005-01333) through the National Research Foundation of Korea (NRF) funded by the Ministry of Education, Science and Technology.

REFERENCES

(1) Stanley, C. J.; Cox, R. B.; Cardosi, M. F.; Turner, A. P. F *J. Immunol. Methods* **1988**, *112*, 153−161.
(2) Porstmann, T.; Kiessig, S. T. *J. Immunol. Methods* **1992**, *150*, 5−21.
(3) Niwa, O. *Electroanalysis* **1995**, *7*, 606−613.
(4) Niwa, O.; Xu, Y.; Halsall, H. B.; Heineman, W. R. *Anal. Chem.* **1993**, *65*, 1559−1563.
(5) Zhu, L.; Anslyn, E. V. *Angew. Chem., Int. Ed.* **2006**, *45*, 1190−1196.
(6) Dhawan, S. *Expert Rev. Mol. Diagn.* **2006**, *6*, 749−760.
(7) Andras, S. C.; Power, J. B.; Cocking, E. C.; Davey, M. R. *Mol. Biotechnol.* **2001**, *19*, 29−44.
(8) Blaedel, W. J.; Boguslaski, R. C. *Anal. Chem.* **1978**, *50*, 1026−1032.
(9) Brakmann, S. *Angew. Chem., Int. Ed.* **2004**, *43*, 5730−5734.
(10) Rosi, N. L.; Mirkin, C. A. *Chem. Rev.* **2005**, *105*, 1547−1562.
(11) Tansil, N. C.; Gao, Z. *Nano Today* **2006**, *1*, 28−37.
(12) Das, J.; Aziz, M. A.; Yang, H. *J. Am. Chem. Soc.* **2006**, *128*, 16022−16023.
(13) Limoges, B.; Marchal, D.; Mavré, F.; Savéant, J. *J. Am. Chem. Soc.* **2006**, *128*, 2084−2092.
(14) Limoges, B.; Marchal, D.; Mavré, F.; Savéant, J. *J. Am. Chem. Soc.* **2006**, *128*, 6014−6015.
(15) Limoges, B.; Marchal, D.; Mavré, F.; Savéant, J.; Schöllhorn, B. *J. Am. Chem. Soc.* **2008**, *130*, 7259−7275.
(16) Limoges, B.; Marchal, D.; Mavré, F.; Savéant, J. *J. Am. Chem. Soc.* **2008**, *130*, 7276−7285.
(17) Das, J.; Jo, K.; Lee, J. W.; Yang, H. *Anal. Chem.* **2007**, *79*, 2790−2796.

(18) Akanda, M. R.; Aziz, M. A.; Jo, K.; Tamilavan, V.; Hyun, M. H.; Kim, S.; Yang, H. *Anal. Chem.* **2011**, *83*, 3926−3933.
(19) Nassef, H. M.; Redondo, M. C. B.; Ciclitira, P. J.; Ellis, H. J.; Fragoso, A.; O'Sullivan, C. K. *Anal. Chem.* **2008**, *80*, 9265−9271.
(20) Wilson, M. S.; Rauh, R. D. *Biosens. Bioelectron.* **2004**, *20*, 276−283.
(21) Thomas, J. H.; Kim, S. K.; Hesketh, P. J.; Halsall, H. B.; Heineman, W. R. *Anal. Chem.* **2004**, *76*, 2700−2707.
(22) Elsholz, B.; Wörl, R.; Blohm, L.; Albers, J.; Feucht, H.; Grunwald, T.; Jürgen, B.; Schweder, T.; Hintsche, R. *Anal. Chem.* **2006**, *78*, 4794−4802.
(23) Kwon, S. J.; Yang, H.; Jo, K.; Kwak, J. *Analyst* **2008**, *133*, 1599−1604.
(24) Feldberg, S. W.; Campbell, J. F. *Anal. Chem.* **2009**, *81*, 8797−8800.
(25) Lövgren, U.; Kronkvist, K.; Johansson, G.; Edholm, L.-E. *Anal. Chim. Acta* **1994**, *288*, 227−235.
(26) Kawashima, T.; Nakano, S.; Tabata, M.; Tanaka, M. *Trends Anal. Chem.* **1997**, *16*, 132−139.
(27) Teshima, N.; Katsumata, H.; Kawashima, T. *Anal. Sci.* **2000**, *16*, 901−911.
(28) Chen, Z.; Zhang, N.; Zhuo, L.; Tang, B. *Microchim. Acta* **2009**, *164*, 311−336.
(29) Savéant, J. *Chem. Rev.* **2008**, *108*, 2348−2378.
(30) Rosokha, S. V.; Kochi, J. K. *Acc. Chem. Res.* **2008**, *41*, 641−653.
(31) Rosokha, S. V.; Kochi, J. K. *J. Am. Chem. Soc.* **2007**, *129*, 3683−3697.
(32) Hubig, S. M.; Rathore, R.; Kochi, J. K. *J. Am. Chem. Soc.* **1999**, *121*, 617−626.
(33) Taube, H.; Myers, H. *J. Am. Chem. Soc.* **1954**, *76*, 2103−2111.
(34) Taube, H. *Angew. Chem., Int. Ed.* **1984**, *23*, 329−339.
(35) Bard, A. J. *J. Am. Chem. Soc.* **2010**, *132*, 7559−7567.
(36) Hamann, T. W.; Ondersma, J. W. *Energy Envirion. Sci.* **2011**, *4*, 370−381.
(37) Peter, L. M. *J. Phys. Chem. Lett.* **2011**, *2*, 1861−1867.
(38) Elsholz, B.; Wörl, R.; Blohm, L.; Albers, J.; Feucht, H.; Grunwald, T.; Jürgen, B.; Schweder, T.; Hintsche, R. *Anal. Chem.* **2006**, *78*, 4794−4802.
(39) Hansen, R. E.; Winther, J. R. *Anal. Biochem.* **2009**, *394*, 147−158.
(40) Eckermann, A. L.; Feld, D. J.; Shaw, J. A.; Meade, T. J. *Coord. Chem. Rev.* **2010**, *254*, 1769−1802.
(41) Chen, P.; McCreery, R. L. *Anal. Chem.* **1996**, *68*, 3958−3965.
(42) Ju, H.; Leech, D. *Phys. Chem. Chem. Phys.* **1999**, *1*, 1549−1554.
(43) Weston, M. C.; Nash, C. K.; Fritsch, I. *Anal. Chem.* **2010**, *82*, 7068−7072.
(44) Shi, M.; Anson, F. C. *Langmuir* **1996**, *12*, 2068−2075.
(45) Das, J.; Lee, J.-A.; Yang, H. *Langmuir* **2010**, *26*, 6804−6808.
(46) Aledo, J. C. *Biochem. Mol. Biol. Educ.* **2007**, *35*, 85−88.
(47) Bauer, C. G.; Eremenko, A. V.; Ehrentreich-Förster, E.; Bier, F. F.; Makower, A.; Halsall, H. B.; Heineman, W. R.; Scheller, F. W. *Anal. Chem.* **1996**, *68*, 2453−2458.
(48) Lee, C.; Shin, D.; Kim, Y. H. *Bull. Korean Chem. Soc.* **1992**, *13*, 449−451.
(49) Asanov, A. N.; Wilson, W. W.; Oldham, P. B. *Anal. Chem.* **1998**, *70*, 1156−1163.
(50) Zudans, I.; Paddock, J. R.; Kuramitz, H.; Maghasi, A. T.; Wansapura, C. M.; Conklin, S. D.; Kaval, N.; Shotoyko, T.; Monk, D. J.; Bryan, S. A.; Hubler, T. L.; Richardson, J. N.; Selisker, C. J.; Heineman, W. R. *J. Electroanal. Chem.* **2004**, *565*, 311−320.
(51) Aziz, M. A.; Park, S.; Jon, S.; Yang, H. *Chem. Commun.* **2007**, *25*, 2610−2612.
(52) Anson, F. C.; Osteryoung, R. A. *J. Chem. Educ.* **1983**, *60*, 293−296.
(53) Bodor, G. S.; Porter, S.; Landt, Y.; Ladenson, J. H. *Clin. Chem.* **1992**, *38*, 2203−2214.
(54) Chunglok, W.; Khownarumit, P.; Rijiravanich, P.; Somasundrum, M.; Surareungchai, W. *Analyst* **2011**, *136*, 2969−2974.
(55) Shen, W.; Tian, D.; Cui, H.; Yang, D.; Bian, Z. *Biosens. Bioelectron.* **2011**, *27*, 18−24.
(56) Zhou, F.; Lu, M.; Wang, W.; Bian, Z.-P.; Zhang, J.-R.; Zhu, J.-J. *Clin. Chem.* **2010**, *56*, 1701−1707.